Boundary-Layer Meteorol (2008) 129:411–430
DOI 10.1007/s10546-008-9316-8

ORIGINAL PAPER

# Hurricane Wind Power Spectra, Cospectra, and Integral Length Scales

**Bo Yu · Arindam Gan Chowdhury · Forrest James Masters**

Received: 22 October 2007 / Accepted: 28 August 2008 / Published online: 24 September 2008


**Abstract** Atmospheric turbulence is an important factor in the modelling of wind forces on structures and the losses they produce in extreme wind events. However, while turbulence in non-hurricane winds has been thoroughly researched, turbulence in tropical cyclones and hurricanes that affect the Gulf and Atlantic coasts has only recently been the object of systematic study. In this paper, Florida Coastal Monitoring Program surface wind measurements over the sea surface and open flat terrain are used to estimate tropical cyclone and hurricane wind spectra and cospectra as well as integral length scales. From the analyses of wind speeds obtained from five towers in four hurricanes it can be concluded with high confidence that the turbulent energy at lower frequencies is considerably higher in hurricane than in non-hurricane winds. Estimates of turbulence spectra, cospectra, and integral turbulence scales presented can be used for the development in experimental facilities of hurricane wind flows and the forces they induce on structures.

**Keywords** Cospectra · Hurricane wind · Integral length scale · Power spectra

## 1 Introduction

Turbulent fluctuations in the surface layer of the atmosphere have a significant effect on wind loads and the losses they produce in high winds. While much research has been performed on turbulence structure, it has largely been concerned with non-hurricane winds; similar investigations for tropical cyclone and hurricane winds have been much less active, owing to the rarity of adequate measurements. The purpose of this paper is to present results of tropical cyclone and hurricane wind speed analyses based on data acquired by the Florida Coastal

B. Yu · A. Gan Chowdhury (✉)
Department of Civil and Environmental Engineering, Engineering Center, EC 3604, Florida International University, 10555 West Flagler Street, Miami, FL 33174, USA
e-mail: chowdhur@fiu.edu

F. J. Masters
Department of Civil and Coastal Engineering, University of Florida, Gainesville, FL, USA

Monitoring Program (FCMP, fcmp.ce.ufl.edu) with a view to contributing new knowledge on turbulence spectra, cospectra, and integral turbulence scales. The FCMP is a consortium of universities formed by Clemson University in 1998 and currently led by the University of Florida.

The basic features of a typical surface wind velocity spectrum were modelled by Van Der Hoven (1957), and showed two major spectral peaks, one at a period corresponding to the passage of large-scale weather systems and one at a period corresponding to micrometeorological scale turbulence. The spectral gap with an approximate time scale of 1 h appears as a large valley separating the two peaks (Stull 1988). Our study is concerned with turbulence on the micrometeorological scale. FCMP data on flow over open terrain and over water are used to estimate spectra and co-spectra of turbulence and integral length scales in the surface layer. The features and limitations of the FCMP records are noted, and estimates based on them are compared with other available estimates.

The paper is organized as follows. Section 2 presents fundamentals pertaining to turbulence on the micrometeorological scale. Sections 3 and 4 describe the hurricane wind speed data being analyzed, and their wind speed characteristics, respectively. Sections 5 and 6 present estimates of the surface roughness lengths around the five selected FCMP tower sites and the integral length scales of the hurricane winds, respectively. Section 7 presents the power spectra and cospectra estimates and comparisons with results obtained by other investigators. Section 8 presents the conclusions of this work.

## 2 Turbulence on the Micrometeorological Scale: Fundamentals

The turbulent energy fluctuations may be viewed as a superposition of eddies, each characterized by a periodic motion of circular frequency $\omega = 2\pi n$, or by a circular wavenumber $k = 2\pi/\lambda$, where $\lambda$ is the wavelength. The total kinetic energy of the turbulent motion may, correspondingly, be regarded as a sum of contributions by each of the eddies of the flow. The function $E(k)$ representing the dependence upon wavenumber of these energy contributions is defined as the energy spectrum of the turbulent motion.

In small eddies, shear deformations, and therefore the viscous stresses, are large. In steady flow the energy fed into the small eddies through inertial transfer from large eddies is balanced by the energy dissipated through viscous effects. The small eddy motion is determined by the rate of energy transfer (or, equivalently, by the rate of energy dissipation, denoted by $\varepsilon$) and by the viscosity. This is known as Kolomogorov's first hypothesis. Since small eddy motion depends only on the internal parameters of the flow, it is independent of external conditions such as boundaries. Therefore local isotropy—the absence of preferred directions of small eddy motion—prevails. It may be further assumed that the energy dissipation is produced almost entirely by the smallest eddies. Thus, at the lowest end of the higher wavenumber range the influence of viscosity is small. In this subrange, known as the *inertial subrange*, the eddy motion may be assumed to be independent of viscosity, and thus determined entirely by the rate of energy transfer, which, in turn, is equal to the rate of energy dissipation. This is Kolmogorov's second hypothesis. In the inertial subrange $E(k)$ depends therefore solely on $k$ and $\varepsilon$, that is,

$$F[E(k),\ k, \varepsilon)] = 0, \tag{1a}$$

and dimensional considerations then yield

$$E(k) = a\varepsilon^{2/3}k^{-5/3} \tag{1b}$$

where $a$ is the Kolmogorov constant, determined experimentally to be $a = 0.5$ (Hinze 1975; Arya 2001). The rate of energy dissipation $\varepsilon$ in a neutral flow is approximately equal to the rate of energy production (see, e.g., Simiu and Scanlan 1996, Sects. 2.3.3 and 2.2.2), that is,

$$\varepsilon = u_*^2 \frac{dU(z)}{dz} \tag{1c}$$

where $U(z)$ is the longitudinal mean speed at $z$, and $u_*$ is the friction velocity (Sect. 5). Equation 1c may be used to deduce information on dissipation rate during hurricane or non-hurricane observations. In a flow with mean speed $U(z)$ it may be assumed that Taylor's hypothesis is valid, that is, $\lambda = U/n$, where $n$ is the frequency in Hz. The circular wavenumber is

$$k = \frac{2\pi n}{U(z)}. \tag{1d}$$

It can be shown (see, e.g., Simiu and Scanlan 1996, p. 57) that, in particular, in neutrally stratified flows Eq. 1b and 1c imply

$$\frac{nS_{uu}(z,n)}{u_*^2} = 0.26 f^{-2/3}, \tag{2a}$$

where $S_{uu}(z,n)$ is the spectral density of the longitudinal velocity fluctuations at height $z$, and

$$f = nz/U(z). \tag{2b}$$

For the low-frequency subrange in neutrally stratified flows the component spectral densities vary in proportion to the square of the friction velocity $u_*$ (Højstrup et al. 1990):

$$S_{aa}\,(n \to 0) \propto u_*^2. \tag{2c}$$

More generally, the one-dimensional velocity spectrum in the neutral surface layer can be written (Kaimal et al. 1972; Teunissen 1980; Olesen et al. 1984; Tieleman 1995):

$$\frac{nS_{aa}\,(n)}{u_*^2} = \frac{A\hat{f}}{\left(1 + B\hat{f}^{\alpha}\right)^{\beta}}, \tag{3}$$

where $aa = (uu, vv, ww)$ and $\hat{f} = n\Lambda/U(z)$, $\Lambda$ is a length scale, e.g., the height $z$ above ground or the longitudinal integral length scale $L_u^x$ at $z$ above the surface, $u, v, w$ are the fluctuating longitudinal, lateral, and vertical velocity components, respectively. For estimates of the coefficients $A$ and $B$ and the exponents $\alpha$ and $\beta$, see Sect. 7.3.

The flow features measured at a point can depend in a complex manner on the surface that affects the flow upwind of that point. A model that reflects that dependence would view the turbulent flux at the point of interest (in practice, at the location of the anemometer) as a sum of contributions by each element of the upwind surface (see, e.g., Horst and Weil 1992). The term "footprint" is used for the contributing surface. For inhomogeneous upwind surfaces a footprint analysis would in principle provide a realistic picture of the turbulent flow features at the point of interest. One appropriate type of analysis involves the solution of the Navier-Stokes equations with boundary conditions based on the actual upwind surface for the case being investigated. In fact, generic analyses of this type, not necessarily referred to as footprint analyses, have been attempted in the past for the simpler problem of estimating flow features downwind of a discrete terrain roughness change (see, e.g., Peterson 1969). Footprint analyses for more complex situations can be based on a variety of methods, all of them fairly laborious, including computational fluid dynamics (CFD). Large-eddy simulations (LES) have been used for some applications, but for turbulence that includes small-scale fluctuations they would not be adequate. According to Foken and Leclerc (2004), validation issues for other existing methods are not fully resolved. Footprint analyses have therefore not been performed in this work and are planned for a subsequent phase of this investigation.

## 3 Hurricane Wind Data Measurements

This study uses surface wind data with 10 Hz resolution collected in real time during hurricane passages to evaluate the wind spectra, cospectra and integral length scales of hurricane winds. To our knowledge, the FCMP data, along with data collected by Texas Tech University (see Schroeder and Smith 2003), are among the first to provide comprehensive information pertaining to tropical cyclone and hurricane winds. 200–27005 Gill 3-dimensional propeller anemometers at 5 and 10 m were used in conjunction with an R. M. Young vane wind monitor (05103 V) at 10 m that determined the direction of the mean wind speed. Data collected were processed in real time by an orthogonalization routine to extract the $u$, $v$, and $w$ components at 5-m and 10-m levels (Masters 2004). The anemometers were calibrated to follow the cosine law within 3% over the ±30-degree range. The measurement system mechanically filters the amplitudes of short wavelength gusts due to the response characteristics of the wind anemometry (Schroeder and Smith 2003), so measurements are accurate only for the lower frequency part of the spectrum. For higher frequencies (e.g., $f = nz/U(z) > 0.2$, see Singer et al. 1968; Teunissen 1970; Fiedler and Panofsky 1970), Kolmogorov similarity may be assumed to hold, so the actual spectral ordinates do not differ from those measured in non-hurricane winds.

We use wind data collected during four hurricane passages from five FCMP observation sites, as follows. *Hurricane Gordon*: tower *Gordon T3*, Honeymoon Island, Florida (28°03′41″N–82°49′44″W) from 1730 UTC on 17 September to 1250 UTC on 18 September 2000. *Hurricane Isidore*: tower *Isidore T2*, Gulf Breeze, Florida (30°21′08″N–87° 10′25.0″W) from 2044 UTC on 26 September to 1136 UTC on 28 September 2002. *Hurricane Lili*: tower *Lili T3*, Lydia, Louisiana (29°54′50″N–91°45′35″W) between 0415 UTC on 3 October and 1802 UTC on 4 October 2002. *Hurricane Ivan*: tower *Ivan T1*, Pensacola Regional Airport, Florida (30°28′45.4″N–87°11′12.8″W) from 2026 UTC on 14 September UTC to 2000 UTC on 16 September 2004, and *Ivan T2*, Fairhope, Alabama (30°28′21.0″N–87°52′30.0″W) from 0053 UTC to 1453 UTC on 16 September 2004, north of the Fairhope Municipal Airport (Figs. 1, 2).

Wind data collected from the five selected FCMP towers were pre-processed and only datasets satisfying quality-control requirements were used. Data pre-processing and quality-control requirements included: (1) separate analyses of hourly record segments with overlapping 15-min segments; (2) decomposition of the records into longitudinal, lateral, and vertical components (data collected were processed in real time by an orthogonalization routine to extract the $u$, $v$, and $w$ components); (3) 10 m s$^{-1}$ at 10-m height was the minimum requirement for segment mean wind speed, to satisfy approximately strong wind and neutral stability conditions; (4) segments with direction shifts larger than 20° were not considered, to avoid records in which wind speeds may correspond to more than one terrain exposure (Masters 2004). For wind directions, see Fig. 1 and Table 1.

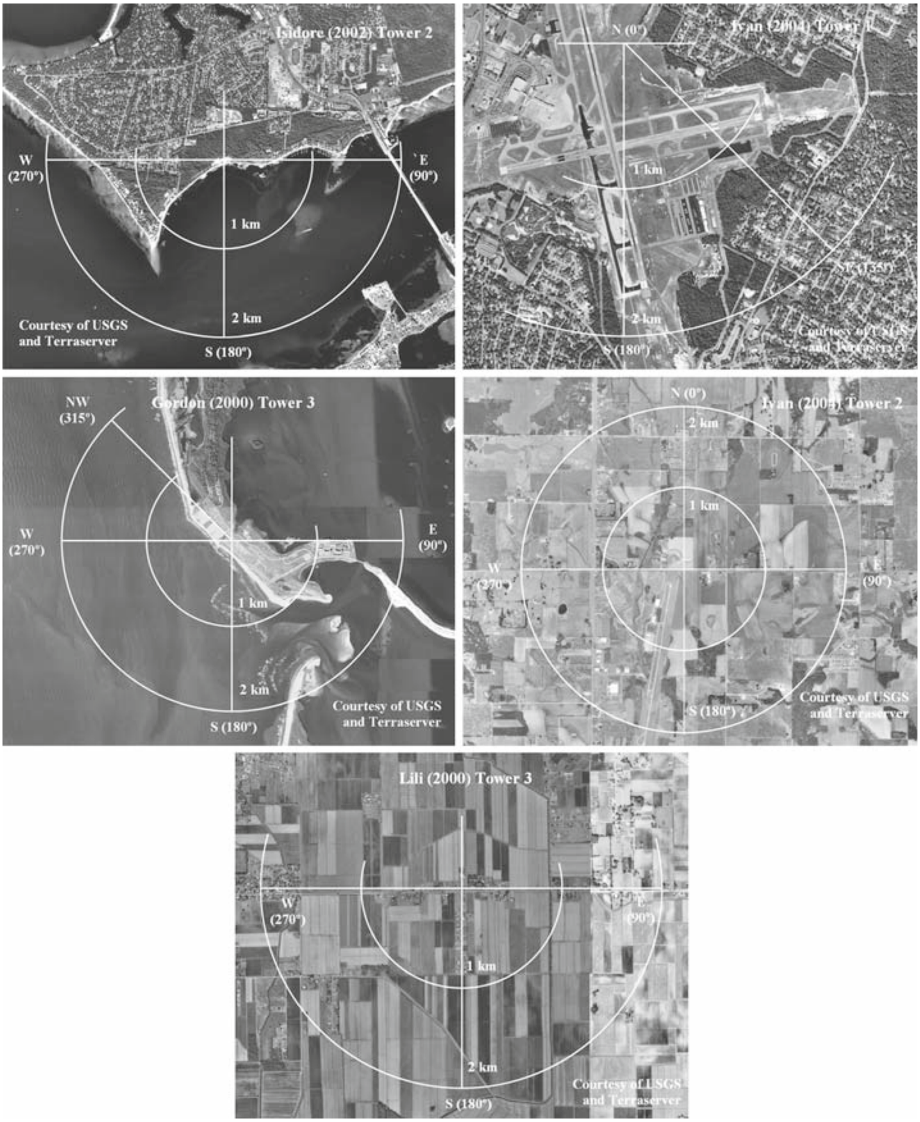


**Fig. 1** FCMP tower sites selected for analysis

## 4 Basic Mean Wind Speeds

The wind direction is measured clockwise from the north. For Isidore T2 and Gordon T3, the wind characteristics are governed by the sea surface roughness upwind of the towers; for Ivan T1, Ivan T2 and Lili T3, they are governed by flat open terrain roughness. The hourly mean wind speeds at 10-m observation height vary from: 12.1 to 17.6 $\mathrm{m\,s^{-1}}$ for Isidore T2; 14.7 to 18.5 $\mathrm{m\,s^{-1}}$ for Gordon T3; 11.1 to 29.9 $\mathrm{m\,s^{-1}}$ for Ivan T1; 15.8 to 24.3 $\mathrm{m\,s^{-1}}$ for Ivan T2; and 11.5 to 22.5 $\mathrm{m\,s^{-1}}$ for Lili T3, see Table 1.

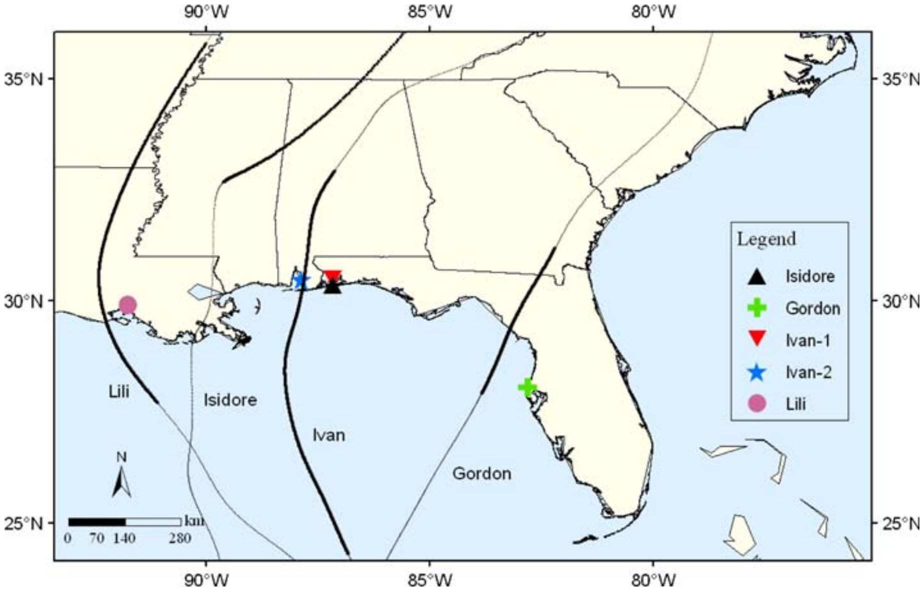


**Fig. 2** Hurricane tracks and FCMP tower locations (bold portions of the tracks indicate measurement periods)

**Table 1** FCMP wind speed and surface roughness

| FCMP tower | | Sea surface | | Flat open land | | |
|---|---|---|---|---|---|---|
| | | Isidore T2 | Gordon T3 | Ivan T1 | Ivan T2 | Lili T3 |
| Wind direction | | (130°, 200°) CW[a] | (180°, 290°) CW[a] | (135°, 240°) CW[a] | (50°, 300°) CW[a] | (145°, 230°) CW[a] |
| Number of segments[b] | | 34 | 18 | 37 | 41 | 27 |
| Hourly wind speed ($\mathrm{m\,s^{-1}}$) | Min | 12.1 | 14.7 | 11.1 | 15.8 | 11.5 |
| | Max | 17.6 | 18.5 | 29.9 | 24.3 | 22.5 |
| | Mean | 14.0 | 17.2 | 19.6 | 18.8 | 15.0 |
| | SD | 1.69 | 0.7 | 5.3 | 2.5 | 3.4 |
| Surface roughness length (m) | Min | 0.0011 | 0.0002 | 0.0080 | 0.0116 | 0.0082 |
| | Max | 0.0060 | 0.0014 | 0.0551 | 0.0497 | 0.0589 |
| | Mean | 0.0027 | 0.0007 | 0.0222 | 0.0257 | 0.0248 |
| | SD | 0.0013 | 0.0004 | 0.0121 | 0.0091 | 0.0147 |

[a] CW: clockwise (e.g., wind direction at Isidore T2 varies counterclockwise from 130° to 200°)
[b] Number of hourly segments (i.e., records of 1-h length) satisfying data quality-control requirements

The observed 3-sec peak gusts on site are 27.1, 29.8, 47.5, 39.9 and 35.8 $\mathrm{m\,s^{-1}}$ for Isidore T2, Gordon T3, Ivan T1, Ivan T2 and Lili T3, respectively. The mean wind speed increased with height for all four hurricanes. Mean wind direction time histories are similar at the two different observation heights (5 and 10 m) for each of the five tower observations.

## 5 Estimation of Surface Roughness Lengths

The flow features are influenced by the underlying terrain roughness. Given the values of the longitudinal turbulence intensity $TI_u$ at height $z$, the logarithmic wind law can be used to estimate the surface roughness length $z_0$ as follows (Wieringa 1993):

$$z_0 = \exp\left(\ln z - \sqrt{\beta}\kappa/TI_u\right) \tag{4}$$

where $\sqrt{\beta} = \sigma_u/u_*$, $\sigma_u$ is the standard deviation of the longitudinal wind component, $u_*$ is the friction velocity, and $\kappa = 0.4$ is the von Karman constant. The friction velocity $u_*$ is

$$u_* = \left(\overline{uw}^2 + \overline{vw}^2\right)^{1/4}, \tag{5}$$

and $u$, $v$, and $w$ are the longitudinal, lateral, and vertical fluctuation components, respectively.

According to Lumley and Panofsky (1964), for a fully developed neutrally stratified flow within the surface layer, $\sqrt{\beta}$ is constant and independent of the underlying terrain roughness. According to Deaves (1981), $\sqrt{\beta} \approx 2.79$ describes adequately fully developed non-hurricane equilibrium flows over open terrain. For Ivan T1, Ivan T2 and Lili T3, the estimated values of $\sqrt{\beta}$ over open terrain are 3.38, 2.85 and 2.72 respectively. For Isidore T2 and Gordon T3, over water they are 3.28 and 3.10, respectively. These estimates are affected by errors, however. For flow over open terrain the ratio between the largest to the smallest value of $\sqrt{\beta}$ is $3.38/2.72 \approx 1.24$; the sample mean is 2.98, the sample standard deviation is 0.35, and the sample coefficient of variation is 0.12; for flow over water the values are $3.28/3.10 \approx 1.06$, 3.19, 0.13, and 0.04, respectively. The variability of $\sqrt{\beta}$ is not surprising, and reflects the fact that, unlike certain fundamental universal constants (e.g., von Kármán's constant), $\sqrt{\beta}$ may well be a parameter whose values differ within limits from storm to storm. In structural engineering applications the variabilities inherent in this and other micrometeorological, climatological, aerodynamics, and mechanical parameters are recognized, and taken into account within a structural reliability framework. It is therefore appropriate to extract from measurements not only typical values of such parameters, but also information on their variability. The coefficients of variation of $\sqrt{\beta}$ appear to be of the same order as corresponding uncertainties in the estimation of $u_*$ (about 10%) reported in the literature for conventional friction velocity measurements (Johnson et al. 1998).

Based on surface wind measurements from the FCMP towers under strong wind conditions, the surface roughness lengths around the tower sites were estimated by using Eq. 4 and wind speeds at 10-m elevation. For the sea surface (Isidore T2 and Gordon T3), the roughness lengths vary from 0.0002 to 0.006 m; for open terrain (Ivan T1, Ivan T2 and Lili T3), the surface roughness lengths vary from 0.0080 to 0.0589 m. Estimated surface roughness lengths around the tower sites and their variability are shown in Table 1. Figure 1 provides visual information on surface roughness conditions and can thus be used to corroborate the classification of terrain exposure for the estimates of friction velocities $u_*$ (Eq. 4) and non-dimensional spectra and cospectra. The estimates of surface roughness lengths and friction velocities are used in Sect. 7. Note, however, that these estimates are subject to errors due primarily to uncertainties in the values of $u_*$. Following Johnson et al. (1998, Eq. 4.16), using for the surface drag coefficient $C_{dn}$ the expression

$$C_{dn} = \{\kappa/[\ln(10/z_0)]\}^2 \tag{6}$$

where $z_0$ is given in m, and neglecting other uncertainties, which are relatively small, the relative uncertainty in $z_0$ is

$$\frac{\Delta z_0}{z_0} \approx -1 + \exp\left\{ -\left(\ln \frac{10}{z_0}\right) \frac{\frac{\Delta u_*}{u_*}}{1 + \frac{\Delta u_*}{u_*}} \right\}. \tag{7}$$

Assuming $\Delta u_*/u_* = 0.10$, for the estimated $z_0 = 0.0002\,\mathrm{m}$, $\Delta z_0/z_0 \approx 2.3$ or $-0.6$, depending on whether $\Delta u_*$ is negative or positive, so $z_0$ can vary between about 0.00007 and 0.0007 m. For the estimated $z_0 = 0.006\,\mathrm{m}$, $z_0$ can vary between about 0.003 m and 0.014 m. For the estimated $z_0 = 0.0589\,\mathrm{m}$, $z_0$ can vary between about 0.04 and 0.10 m.

It is of interest to compare the estimated roughness lengths estimated in this work for flow over water with those estimated from the data originating in the RASEX field campaigns. The data, recorded over 30 min at a 20-Hz sampling rate, were obtained by a sonic anemometer mounted at 3-m above mean sea level on a tower situated in 4-m water depth with an upstream fetch of 15–20 km in a 90-degree sector with upstream water depths of 5–20 m (Johnson et al. 1998). However, the mean speeds were measured by a cup anemometer at 7 m, with an estimated accuracy of about 2%. The mean speeds at the standard 10-m height were obtained from the speeds at 7-m height by using a power law with exponent 1/7. This assumption is commonly used for mean speeds over open terrain, and implies $z_0 \approx 0.03\,\mathrm{m}$, see, e.g., Simiu and Scanlan (1996). Since over water $z_0$ can vary between about 0.0001 and 0.001 m, the use of the power law by Johnson et al. (1998) entails a systematic error comparable to the errors in the anemometer measurements. The estimated roughness lengths were about 0.0001 to 0.0015 m, with no clear dependence on wind speed, versus about 0.0002 to 0.006 m in this study.

The FCMP towers are not equipped to monitor wave direction. For this reason no analysis was performed in this study of the role of wave direction, which may have caused the high values of $z_0$ for Isidore T2. It is the authors' recommendation that the requisite information on waves be provided in future hurricane wind speed measurement campaigns.

## 6 Estimation of Integral Length Scales

Atmospheric turbulence affects the aerodynamic response of structures in general and the dynamic response of flexible structures in particular (see, e.g., Simiu and Scanlan 1996). Integral scales of turbulence are measures of the average size of the turbulent eddies of the flow, with the longitudinal integral length scale ($L_u^x$) defined as:

$$L_u^x = U \int_0^\infty \rho_{uu}(\tau)\, d\tau, \tag{8}$$

where $U$ is the mean wind speed, $\tau$ is the time lag, and $\rho_{uu}$ is the autocorrelation coefficient function of the longitudinal wind component, defined as:

$$\rho_{uu}(\tau) = \frac{E\left[\{u(t) - U\}\{u(t+\tau) - U\}\right]}{\sigma_u^2} \tag{9}$$

where $E[\phi(t)]$ is the expected value of the stationary random process $\{\phi(t)\}$. Large values of $L_u^x$ imply large autocorrelations $\rho_{uu}(\tau)$, meaning that the fluctuating velocity $u(x, y, z)$ is well correlated with the velocity $u(x + \Delta x, y, z)$ for large $\Delta x$; that is, in the undisturbed wind field, for any time $t$ fluctuating speeds at $x$ and $x + \Delta x$ are close to each other.

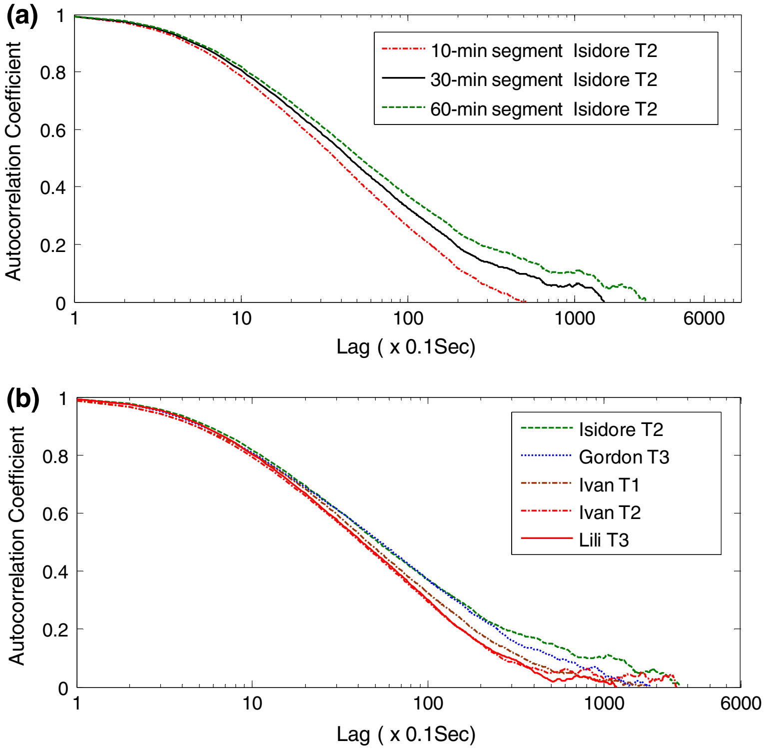


**Fig. 3** (**a**) Variation of autocorrelation coefficient with segment length at 10-m elevation for Isidore T2; (**b**) Autocorrelation coefficient based on 1-h wind speed segments at 10-m elevation at five selected FCMP sites

Estimates of both $\rho_{uu}$ and $L_u^x$ values depend upon the length of the record being analyzed. For Isidore T2, the variations of $\rho_{uu}$ as a function of the lag time $\tau$ (in seconds) at 10-m height for different segment lengths (10, 30, and 60 min) are shown in Fig. 3a. Analyses of Gordon T3, Ivan T1, Ivan T2 and Lili T3 indicate similar results. Figure 3b shows the variations of $\rho_{uu}$ at 10-m height with lag time $\tau$, based on 1-h segment lengths for Isidore T2, Gordon T3, Ivan T1, Ivan T2 and Lili T3.

In theory, the definition of the integral length scale pertains to an infinitely long record. In practice, since the record lengths are limited, the largest wind speed record over which the wind is stationary (in this case 60 min) provides the physically most relevant estimate of the length scale.

For the five selected FCMP observation sites, estimates of $L_u^x$ for various segment lengths are shown in Table 2. As expected, the longitudinal length scale increases with segment length. At a 10-m observation height, the 10-min longitudinal integral length scales are 140, 176, 154, 123 and 94 m and 1-h mean values are 450, 365, 240, 366 and 226 m for Isidore T2, Gordon T3, Ivan T1, Ivan T2 and Lili T3, respectively. We note that length scales are typically larger over the sea (Isidore T2 and Gordon T3) than over open terrain (Ivan T1, Ivan T2 and Lili T3). The length scales vary from hurricane to hurricane, the ratio between the largest to the smallest length scale for 10-m elevation and a 60-min time interval being $450/365 \approx 1.2$ for flow over the sea, and $366/226 \approx 1.6$ for flow over open terrain. A linear regression was applied to fit the variations of $L_u^x$ with different average segment lengths, as shown in Fig. 4. The resulting fitted curve is:

**Table 2** Longitudinal integral length scales at 5-m and 10-m elevations; unit: m

| Tower site | Anemometer height | 5 min | 10 min | 20 min | 30 min | 40 min | 50 min | 60 min |
|---|---|---|---|---|---|---|---|---|
| Isidore T2 (sea surface) | 5 m | 71 | 98 | 148 | 204 | 246 | 257 | 312 |
| | 10 m | 98 | 140 | 205 | 304 | 358 | 385 | 450 |
| Gordon T3 (sea surface) | 10 m | 108 | 176 | 223 | 266 | 281 | 330 | 365 |
| Ivan T1 (open land) | 5 m | 95 | 126 | 145 | 165 | 170 | 182 | 197 |
| | 10 m | 115 | 154 | 180 | 205 | 209 | 224 | 240 |
| Ivan T2 (open land) | 5 m | 88 | 105 | 134 | 134 | 161 | 213 | 314 |
| | 10 m | 102 | 123 | 154 | 162 | 186 | 282 | 366 |
| Lili T3 (open land) | 5 m | 67 | 82 | 95 | 107 | 122 | 147 | 189 |
| | 10 m | 79 | 94 | 116 | 134 | 151 | 182 | 226 |

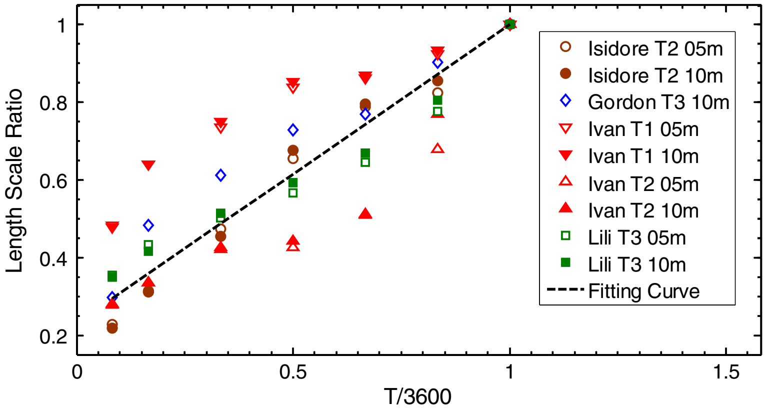


**Fig. 4** Integral length scale ratios ($L_u^x(T)/L_u^x(3600)$) based on different record length ratios $T/3600$ ($T$ in seconds)

$$L_u^x(T)/L_u^x(3600) = 0.23 + 0.77T/3600 \tag{10}$$

where $T$ is the average segment length in seconds. The longitudinal length scale increases with the observational height as shown in Table 2 and Fig. 5. The ratios of the integral length scale at 5-m observational height to the integral scale at 10 m are 0.695 and 0.83 for flow over the sea and over open terrain, respectively.

## 7 Power Spectra and Cospectra: Estimation and Variability

For real-valued stationary signals, power spectral and cospectral functions describe the power distributions of the time series in the frequency domain. For our data, they were computed by the Welch method based on the direct Fast Fourier Transforms (FFT) of the original stationary signals and described in detail by Bendat and Piersol (2000). The Hanning window was used to suppress the side-lobe leakage. The power spectra and cospectra are estimated by averaging the respective power spectra and cospectra based on the individual 1-h wind speed segments. In this section, power spectra and cospectra of velocity fluctuations in the surface layer are estimated and modelled, and are compared with results and models available in the literature.

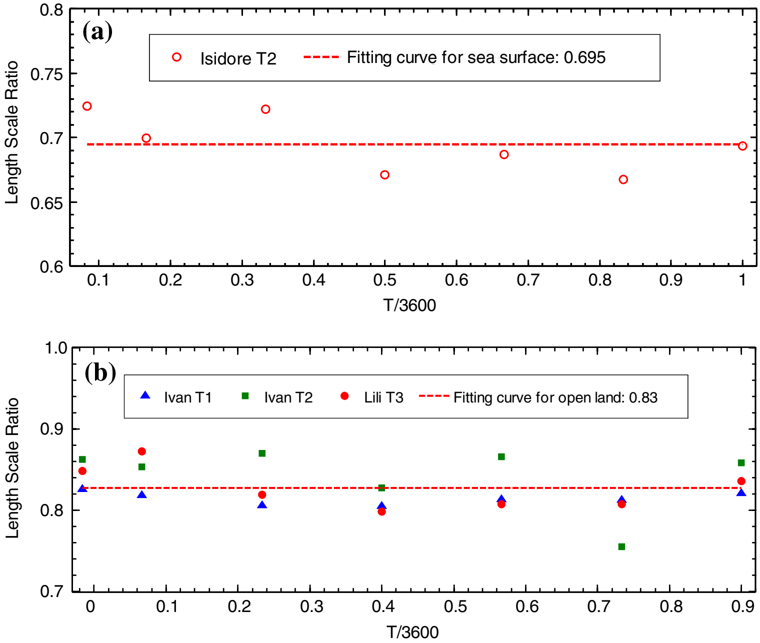


**Fig. 5** Ratios of the integral length scales at 5-m elevation to those at 10-m elevation based on different record length ratio $T/3600$ ($T$ in seconds)

## 7.1 Wind Spectra and Cospectra over Surfaces with Various Roughness Lengths

Wind spectra and cospectra are affected by the upstream roughness length, and estimates of roughness lengths in Sect. 5 were used to stratify the observed wind spectra and cospectra into two roughness regimes, $0.0002\,\text{m} \le z_0 \le 0.006\,\text{m}$ corresponding to the sea surface, and $0.008\,\text{m} \le z_0 \le 0.06\,\text{m}$ corresponding to open terrain. Figure 2 shows hurricane tracks and FCMP tower locations with bold portions of the tracks indicating measurement periods for which the spectra and cospectra have been estimated. Figure 6 presents the estimated power spectra at 10-m elevation for open terrain ($0.008\,\text{m} \le z_0 \le 0.06\,\text{m}$, for Ivan T1, Ivan T2 and Lili T3). The resulting fitted curves, as well as mean curves, for power spectra of longitudinal ($u$), lateral ($v$) and vertical ($w$) wind components at 10-m height over open terrain are plotted in Fig. 7.

The square of the friction velocity $u_*$ and the frequency $n$ were used to normalize the power spectral densities, and the observational height $z$ and mean wind speed $U(z)$ were used to normalize the frequency $n$, giving the reduced frequency as $f = nz/U$. It was found that the estimated power spectra fall faster at high frequencies than the spectra yielded by Kolmogorov theory. The lack of high-frequency energy is due to the response characteristics of the wind anemometry, which mechanically filters the amplitudes of short wavelength gusts. For this reason, as was noted earlier, the FCMP data are useful only for the lower frequency part of the spectrum.

For the sea surface, the normalized power spectral values for longitudinal wind components from Isidore T2 are higher than those from Gordon T3. For example, for $f = 0.01$, the ratio of the Isidore T2 to the Gordon T3 power spectral energy is $2.15/1.75 \approx 1.23$ for

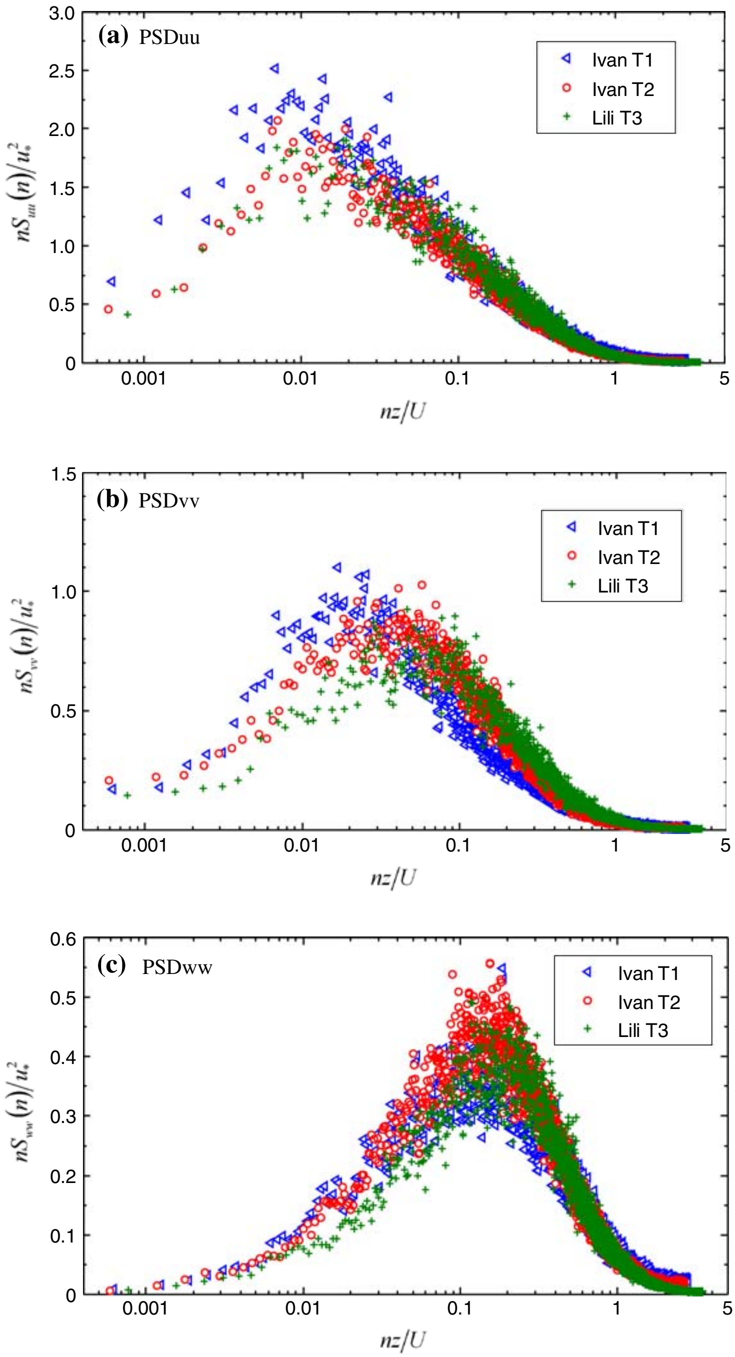


**Fig. 6** Wind spectra at 10-m elevation over open terrain

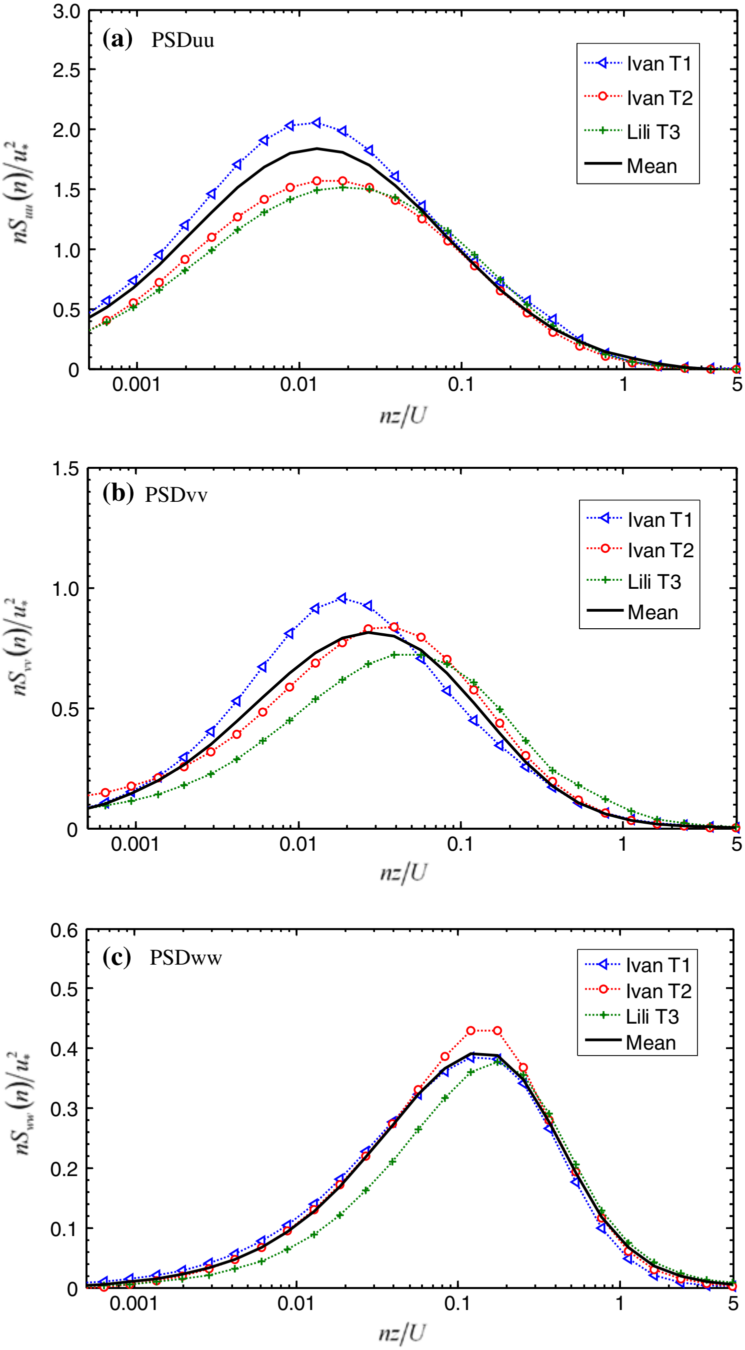


**Fig. 7** Fitted curves of wind spectra at 10-m elevation over open terrain

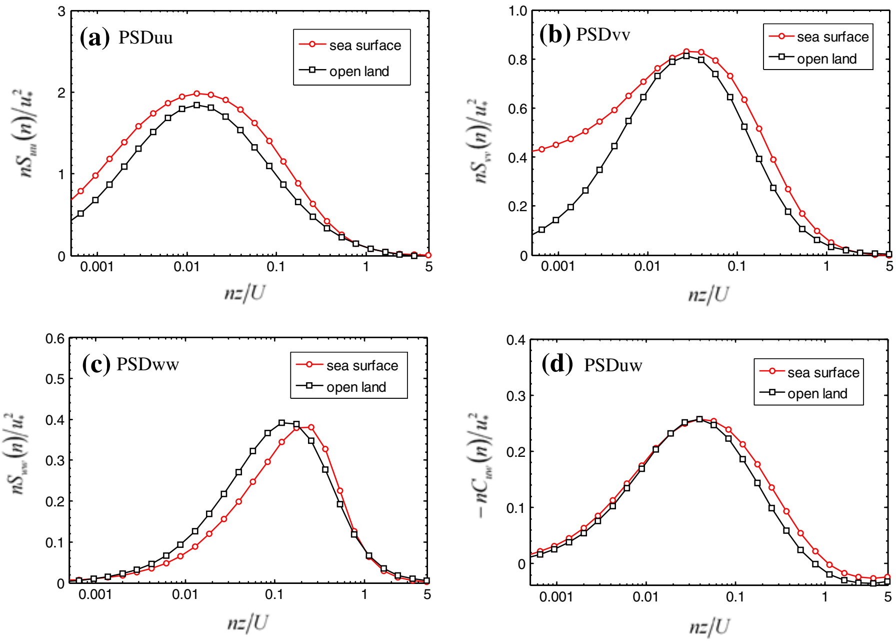


**Fig. 8** Wind spectra and cospectra at 10-m elevation for terrains with various roughness lengths

the longitudinal component. The differences between the spectra do not appear to be related to the respective roughness lengths (see Table 1).

For open terrain, Figs. 6 and 7 show that the normalized power spectral values for the longitudinal and lateral wind components from Ivan T1 are higher than those from Ivan T2 and Lili T3 for $f < 0.02$. For example, for $f = 0.01$, the ratio of the largest to the smallest power spectral energy is $2.08/1.47 \approx 1.42$ for the longitudinal component and $0.82/0.48 \approx 1.71$ for the lateral component, as shown in Fig. 7.

Wind spectra and cospectra for flow over water and over open terrain are shown in Fig. 8. Spectral values for the longitudinal and lateral wind components for winds over the sea are higher than for winds over open flat terrain. For example, for the longitudinal power spectra $S_{uu}$, the normalized spectral peaks over the sea surface and over open terrain were 2.0 and 1.8, respectively, that is, the ratio of the peaks was $2.0/1.8 \approx 1.11$; similar results were found for the lateral power spectra $S_{vv}$. The spectra of the vertical wind component and the $uw$ cospectral values over the sea are comparable to values over open terrain, as shown in Fig. 8.

## 7.2 Wind Spectra and Cospectra for Various Observational Heights and Wind Speeds

The estimated power spectra and cospectra based on 1-h wind speed segments at 10-m and 5-m elevations are shown in Fig. 9 for open exposure with roughness lengths $0.008\,\text{m} \le z_0 \le 0.06\,\text{m}$ (see Table 1). Estimates of the normalized power spectra at 5-m height are larger than those at 10-m height for longitudinal (for $f < 0.02$) and lateral wind components. However, differences are smaller for vertical wind spectra and $uw$ cospectra.

To investigate the effects of wind speed on the variation of the normalized power spectra and cospectra of hurricane winds, the estimated power spectra and cospectra at 10-m

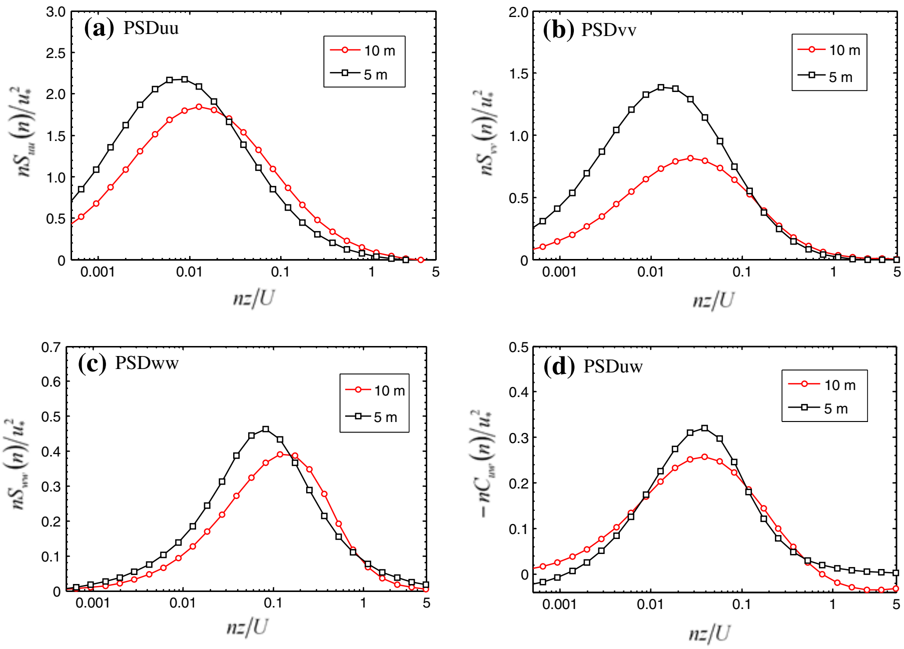


**Fig. 9** Variation of wind spectra and cospectra with observational height

elevation for open exposure were separated for two mean wind speed ranges, $10 \le U \le 20\,\mathrm{m\,s^{-1}}$ and $20 \le U \le 30\,\mathrm{m\,s^{-1}}$. The estimated power spectra and cospectra of hurricane wind fluctuations are comparable for different regimes, as expected.

## 7.3 Comparison of Estimated Power Spectra and Cospectra with Estimates Reported by Other Investigators

In this section, the estimated power spectra and cospectra based on 1-h wind speed segments at 10-m height over open exposure ($0.008\,\mathrm{m} \le z_0 \le 0.06\,\mathrm{m}$) are compared to the wind spectra and cospectra obtained for non-hurricane winds by Lumley and Panofsky (1964); Kaimal et al. (1972) and Tieleman (1995). The spectral models for the neutral atmospheric surface layer are mostly of the general form of Eq. 3 and are shown in Table 3. Equations and coefficients for spectra and cospectra based on the analyses presented in this paper are given in Appendix A and Table 4, respectively.

For power spectra of the longitudinal velocity component, $S_{uu}$, Fig. 10a shows the normalized longitudinal velocity spectra $nS_{uu}(n)/u_*^2$ as a function of reduced frequency $f$. Compared with the Tieleman and revised Kaimal curves, the estimated mean spectrum for hurricane wind has significantly more energy at lower frequencies ($f < 0.02$, say), with the estimated normalized spectral peak of about 1.8, higher than the value of 1.3 from the revised Kaimal model.

For power spectra of the lateral velocity component, $S_{vv}$, and power spectra of the vertical velocity component, $S_{ww}$, the normalized spectra are plotted in Fig. 10b and c. Similar to the longitudinal velocity spectrum, the estimated spectra of $S_{vv}$ and $S_{ww}$ for hurricane winds have more energy at lower frequencies than the referenced models for non-hurricane

**Table 3** Spectral models for the neutral non-hurricane atmospheric surface layer

| Formula | Author(s) | Notes |
|---|---|---|
| $\frac{nS_{uu}(n)}{u_*^2} = \frac{200f}{(1+50f)^{5/3}}$ | Kaimal et al. (1972), corrected for low frequency[a] | $u$-component |
| $\frac{nS_{uu}(n)}{u_*^2} = \frac{252.6f}{(1+60.62f)^{5/3}}$ | Tieleman (1995) | $u$-component, blunt model for perturbed terrain |
| $\frac{nS_{uu}(n)}{u_*^2} = \frac{128.28f}{1+475.09f^{5/3}}$ | Tieleman (1995) | $u$-component, point model for FSU[b] |
| $\frac{nS_{vv}(n)}{u_*^2} = \frac{15f}{(1+9.5f)^{5/3}}$ | Kaimal et al. (1972) | $v$-component |
| $\frac{nS_{vv}(n)}{u_*^2} = \frac{53.76f}{(1+20.16f)^{5/3}}$ | Tieleman (1995) | $v$-component, blunt model for perturbed terrain |
| $\frac{nS_{vv}(n)}{u_*^2} = \frac{27.3f}{1+75.84f^{5/3}}$ | Tieleman (1995) | $v$-component, point model for FSU |
| $\frac{n.S_{ww}(n)}{u_*^2} = \frac{3.36f}{1+10f^{5/3}}$ | Lumley and Panofsky (1964) | $w$-component |
| $\frac{nS_{ww}(n)}{u_*^2} = \frac{2f}{1+5.3f^{5/3}}$ | Kaimal et al. (1972) | $w$-component |
| $\frac{nS_{ww}(n)}{u_*^2} = \frac{5.13f}{(1+4.92f)^{5/3}}$ | Tieleman (1995) | $w$-component, blunt model for perturbed terrain |
| $\frac{nS_{ww}(n)}{u_*^2} = \frac{2.604f}{1+7.232f^{5/3}}$ | Tieleman (1995) | $w$-component, point model for FSU |

[a] Simiu and Scanlan (1996, p. 59). The correction augmented the lower frequency spectral components so that the r.m.s.$(u) = 2.45u_*$

[b] FSU, Flat, smooth and uniform terrain

winds. It follows that, according to the estimates presented in this study, the low-frequency energy content is significantly higher for hurricane than for non-hurricane winds. This result is consistent with results obtained for one hurricane record (Hurricane Bonnie) by Schroeder and Smith (2003).

Based on Kansas experiments, Kaimal et al. (1972) proposed a model for the power cospectrum $C_{uw}$ of the longitudinal and the vertical components for non-hurricane winds given by Eq. 11:

$$\frac{-nC_{uw}(n)}{u_*^2} = \frac{14f}{(1+9.6f)^{2.4}}. \tag{11}$$

The estimated $uw$ cospectrum $C_{uw}$ based on the FCMP records is compared with the Kaimal model (Eq. 11), and the observed normalized peak value of 0.25 is lower than the Kaimal value of 0.45. The reduced frequency of 0.04 corresponding to the observed cospectrum peak is also lower than the value of 0.15 in the Kaimal model. As indicated earlier, estimates of high-frequency spectral components for the FCMP records are not accurate owing to the properties of the Young anemometers used in the measurements.

## 8 Conclusions

Using surface wind measurements collected by FCMP towers (Isidore T2, Gordon T3, Ivan T1, Ivan T2 and Lili T3) during the passage of hurricane, we calculated the power spectra

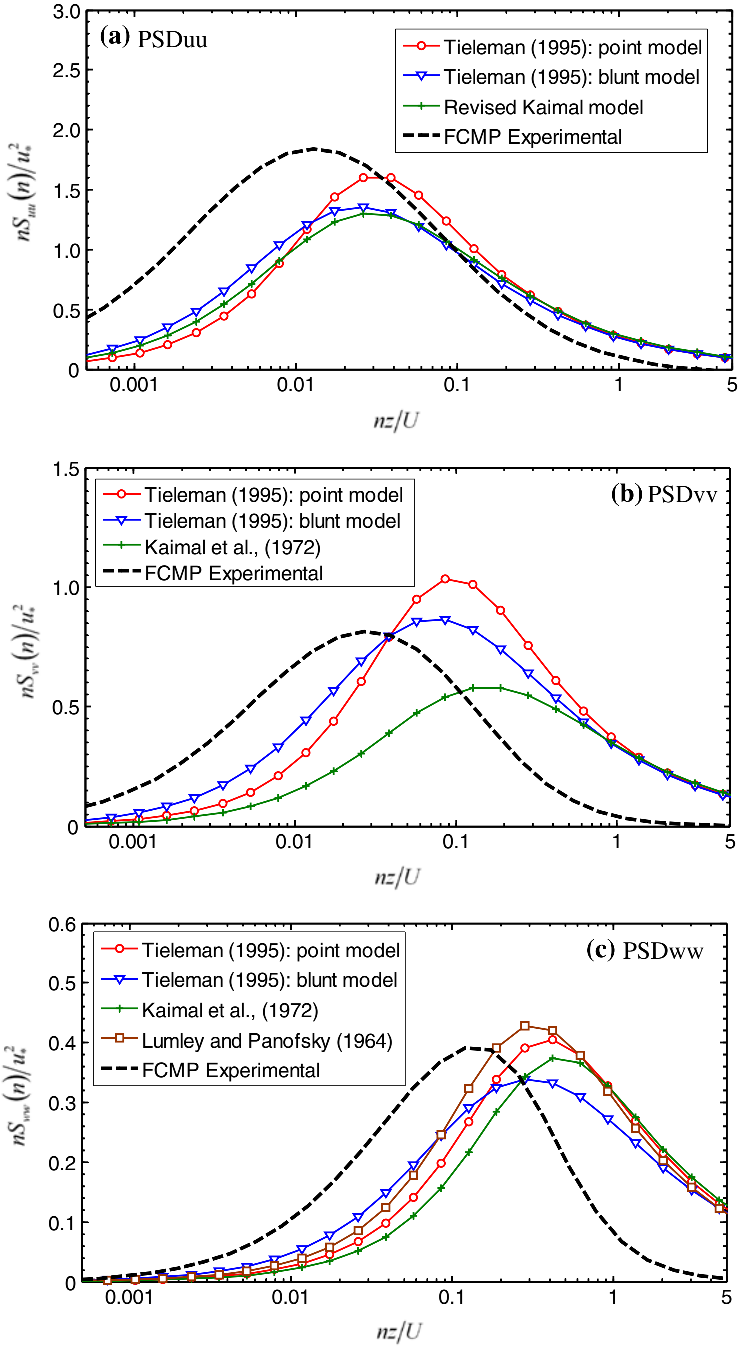


**Fig. 10** (**a**) Longitudinal wind spectra estimation and comparison at 10-m elevation; (**b**) Lateral wind spectra estimation and comparison at 10-m elevation; (**c**) Vertical wind spectra estimation and comparison at 10-m elevation

and cospectra, and turbulence integral length scales, of tropical cyclone and hurricane winds over coastal areas under neutral conditions. The conclusions are:

(1) Compared with power spectral models proposed by other investigators for non-hurricane winds, the observed normalized power spectra of longitudinal, lateral and vertical hurricane wind components have significantly more energy at lower frequencies. This is in agreement with results obtained for one hurricane record by Schroeder and Smith (2003). For $uw$ cospectra, the observed cospectral peaks and the corresponding reduced frequency are lower than the values obtained by Kaimal et al. (1972).

(2) Values of power spectra of longitudinal and lateral wind components over the sea were higher than those over open terrain, while the spectra of the vertical wind component and the $uw$ cospectral values over the two surface regimes were comparable.

(3) Typically, values of power spectra and cospectra of hurricane winds at 5-m elevation were larger than those at 10-m elevation, while value of power spectra and cospectra are comparable for different wind speeds.

(4) Results showed that the longitudinal length scales increase with segment length and elevation. Typically, the longitudinal length scales are lower over open terrain than over the sea surface. The ratios between the largest and smallest estimated integral turbulence scales at 10-m elevation were about 1.2 and 1.6 for the sea surface and open terrain, respectively.

(5) The ratio between the largest to the smallest value of the turbulence parameter $\sqrt{\beta}$ was approximately 1.06 for the sea surface and 1.24 for open terrain. The variabilities of non-dimensional power spectra are approximately commensurate with the squares of these ratios for all turbulent fluctuations.

The work presented herein, among the first devoted to estimating near-surface flow characteristics in tropical cyclones and hurricanes, would not have been possible without the surface measurements obtained, and provided to the authors, by the Florida Coastal Management Program (FCMP). These data did not include information on waves occurring in ocean areas from which winds measured at the towers originated, and in particular on the direction of the waves. Improvements upon the results obtained in this study could be achieved by accounting for wave data. For this reason it is recommended that FCMP or similar measurement programs on hurricane to be conducted in the future include the requisite information on waves.

**Acknowledgements** The authors gratefully acknowledge the Florida Coastal Monitoring Program (FCMP, fcmp.ce.ufl.edu) for providing hurricane surface-wind measurements for this study.

## Appendix A: Coefficients of Power Spectra and Cospectra of Hurricane Winds Based on FCMP Dataset

The spectra and cospectra estimated from the FCMP dataset were used to develop a series of power spectral curves for hurricane winds. Second power numerator and third power denominator polynomials fit the observed spectra and cospectra best, that is,

$$\frac{nS_{aa}}{u_*^2} = \frac{p_1 f^2 + p_2 f + p_3}{f^3 + q_1 f^2 + q_2 f + q_3}, \tag{12}$$

where $a = u, v, w$,

$$\frac{nC_{uw}}{u_*^2} = \frac{p_1 f^2 + p_2 f + p_3}{f^3 + q_1 f^2 + q_2 f + q_3}, \tag{13}$$

**Table 4** Coefficients of power spectra and cospectra of hurricane winds

| Spectra/Cospectra | $p_1$ | $p_2$ | $p_3$ | $q_1$ | $q_2$ | $q_3$ |
|---|---|---|---|---|---|---|
| $S_{uu}$, 10 m, over land | −0.9999 | 3.112 | 1.159e-4 | 18.64 | 1.188 | 3.35e-3 |
| $S_{vv}$, 10 m, over land | 0.006089 | 0.0496 | 7.7789e-7 | 0.321 | 0.04105 | 2.914e-4 |
| $S_{ww}$, 10 m, over land | 0.005569 | 0.1005 | −1.742e-5 | 0.1465 | 0.16 | 7.911e-3 |
| $C_{uw}$, 10 m, over land | −0.3493 | 0.2655 | −3.63e-5 | 4.253 | 0.6107 | 7.725e-3 |
| $S_{uu}$, 10 m, sea | −0.00598 | 0.1544 | 1.055e-5 | 0.4458 | 0.06486 | 9.754e-5 |
| $S_{vv}$, 10 m, sea | −0.07044 | 0.2392 | 8.606e-4 | 1.023 | 0.2151 | 2.2212e-3 |
| $S_{ww}$, 10 m, sea | −0.001399 | 0.07417 | 2.159e-5 | −0.2446 | 0.1565 | 8.869e-3 |
| $C_{uw}$, 10 m, sea | −0.2359 | 0.2563 | −1.482e-5 | 2.652 | 0.6884 | 6.424e-3 |
| $S_{uu}$, 5 m, over land | −0.554 | 1.088 | 2.637e-5 | 10.74 | 0.3311 | 6.432e-4 |
| $S_{vv}$, 5 m, over land | −0.02819 | 0.06354 | 4.433e-6 | 0.5482 | 0.02852 | 1.292e-4 |
| $S_{ww}$, 5 m, over land | 0.08929 | 6.398e-4 | −1.461e-7 | 0.03725 | 0.0071 | 2.348e-5 |
| $C_{uw}$, 5 m, over land | 0.01101 | 0.003692 | −4.327e-6 | 0.05004 | 0.006325 | 1.069e-4 |
| $S_{uu}$, 5 m, sea | −0.04735 | 0.05843 | 6.077e-6 | 0.1612 | 0.01368 | 3.595e-5 |
| $S_{vv}$, 5 m, sea | −0.02935 | 0.06722 | 2.861e-4 | 0.3774 | 0.03607 | 4.799e-4 |
| $S_{ww}$, 5 m, sea | −0.00267 | 0.01798 | −1.295e-5 | −0.1006 | 0.03082 | 1.014e-3 |
| $C_{uw}$, 5 m, sea | −0.01065 | 0.005406 | −7.23e-6 | −0.04522 | 0.01241 | 1.058e-4 |

where $f$ is the reduced frequency defined earlier, and $n$ is the frequency in Hz. In the limit of large $f$ the right-hand sides of Eqs. 12 and 13 are proportional to $f^{-2/3}$, as may be assumed for $f > 0.2$ (Singer et al. 1968; Teunissen 1970; Fiedler and Panofsky 1970). Table 4 presents the coefficients $p_i$ and $q_i (i = 1, 2, 3)$ for power spectra and cospectra of hurricane wind components at two observational heights and for the sea surface and open terrain under near-neutral conditions. The estimates of the non-dimensionalized spectra at various non-dimensional frequencies differ from the best-fitting spectral curve by an amount that is typically of the order of 10% of the spectral ordinate, except for high frequencies where the differences can be larger.

## References


Arya SP (2001) Introduction to micrometeorology, 2nd edn. Academic Press, 450 pp

Bendat JS, Piersol AG (2000) Random data analysis and measurement procedures, 3rd edn. Wiley, 594 pp

Deaves DM (1981) Terrain-dependence of longitudinal RMS velocities in the neutral atmosphere. J Wind Eng Ind Aerodyn 8:259–274

Fiedler F, Panofsky HA (1970) Atmospheric scales and the spectral gap. Bull Am Meteorol Soc 51:114–1119

Foken T, Leclerc MY (2004) Methods and limitations in validation of footprint models. Agric For Meteorol 127:223–234

Hinze JO (1975) Turbulence, 2nd edn. McGraw-Hill, New York, 790 pp

Højstrup J, Larsen SE, Madsen PH (1990) Power spectra of horizontal wind components in the neutral atmospheric surface boundary layer. In: Ninth symposium on turbulence and diffusion, AMS, pp 305–308

Horst TW, Weil JC (1992) Footprint estimation for scalar flux measurements in the atmospheric surface layer. Boundary-Layer Meteorol 59:279–296

Johnson HK, Højstrup J, Vested HJ, Larsen SE (1998) On the dependence of sea surface roughness on wind waves. J Phys Oceanogr 28:1702–1716

Kaimal JC, Wyngaard JC, Izumi Y, Coté OR (1972) Spectral characteristics of surface-layer turbulence. Quart J Roy Meteorol Soc 98:563–598

Lumley JL, Panofsky HA (1964) The structure of atmospheric turbulence. Wiley, New York, 239 pp

Masters FJ (2004) Measurement, modeling and simulation of ground-level tropical cyclone winds. PhD dissertation, University of Florida

Olesen HR, Larsen SR, Hestrup J (1984) Modeling velocity spectra in the lower part of the planetary boundary layer. Boundary-Layer Meteorol 29:285–312

Peterson EW (1969) Modification of mean flow and turbulent energy by a change in surface roughness under conditions of neutral stability. Quart J Roy Meteorol Soc 95:561–575
Schroeder JL, Smith DA (2003) Hurricane Bonnie wind flow characteristics as determined from WEMITE. J Wind Eng Ind Aerodyn 91:767–789
Simiu E, Scanlan R (1996) Wind effects on structures, 3rd edn. Wiley, New York, 704 pp
Singer IA, Busch NE, Frizzola JA (1968) The micrometeorology of the turbulent flow field in the atmospheric boundary surface layer. In: Proceedings of international research seminar on wind effects on buildings and structures, Ottawa, University of Toronto Press, vol 1, pp 557–594
Stull RB (1988) An introduction to boundary layer meteorology. Kluwer Academic Publishers, Dordrecht, 666 pp
Teunissen HW (1970) Characteristics of the mean wind and turbulence in the planetary boundary layer, Review No. 32, Institute for Aerospace Studies, University of Toronto
Teunissen HW (1980) Structure of mean winds and turbulence in the planetary boundary layer over rural terrain. Boundary-Layer Meteorol 19:187–221
Tieleman HW (1995) Universality of velocity spectra. J Wind Eng Ind Aerodyn 56:55–69
Van Der Hoven (1957) Power spectrum of horizontal wind speed in the frequency range from 0.0007 to 900 cycles per hour. J Meteorol 14:160–164
Wieringa J (1993) Representative roughness parameters for homogeneous terrain. Boundary-Layer Meteorol 63:323–363